Research Journal of Engineering Sciences ISSN 2278 – 9472
Vol. **7(1),** 1-10, January **(2018)** *Res. J. Engineering Sci.*

Minimization of discretization errors and boundary mismatch problems in numerical analyses through h-adaptive mesh generation and multi-edge concept

Komla Kpogli[1], Sibiri Wourè-Nadiri Bayor[1*], E. Ouro-Djobo Samah[2], Kokou Tcharie[3] and Arnulf Kost[4]
[1]Departement of Electrical Engineering, Ecole Nationale Supérieured'Ingénieurs (ENSI), Université de LOME, Togo
[2]Centre de la Construction et du Logement (CCL), Cacavelli, Lome, Togo
[3]Departement of Mathematics, Faculté des Sciences (FDS), Université de LOME, Togo
[4]Lehrstuhl Allgemeine Elektrotechnik und Numerische Feldberechung, TU Cottbus, Postfach 101344, D-03013 Cottbus, Germany
bayores1@yahoo.fr

Available online at: www.isca.in, www.isca.me
Received 28th September 2017, revised 12th January 2018, accepted 24th January 2018

Abstract

In any analysis of practical problem using Finite Element Method (FEM), discretization errors are intentionally introduced which most of the time lead to boundary mismatch problems in curved areas where boundary condition of a third kind is applied. In this paper linear finite elements approach with a Multi-Edge concept and h-Adaptive mesh generation have been proposed to minimize the numerical errors.

Keywords: h-adaptive, discretisation-error, boundary-mismatch, multi-Edge, d-Simplex-subdivision.

Introduction

In general truncation or discretization errors, rounded-off in precision and approximations in the mathematical model of a real problem are errors which arise in the approximate numerical solutions[1].Modelling errors arising mainly from chosen shape functions should be kept as low as possible in any finite element analysis to obtain solutions close to the exact solution[1,2].

In this paper, we analyse this problem using local error estimation, the h-adaptive mesh and the Multi-Edge concept. And as examples the magneto-thermal transient phenomena have been taken into consideration.

Localized error determination

The localized error e_i (x, y, z) at any point i (x, y, z) in a medium, where a physical phenomenon is taking place, is normally defined as the difference between the exact solution U (x, y, z) and the approximate one $\overline{U}(x, y, z)$ obtained by the finite element method:

$$e_i(x,y,z) = \left|U(x,y,z) - \overline{U}_n(x,y,z)\right| \to 0, \text{ if } n \to \infty \quad (1)$$

Where the degree of freedom of $\overline{U}_n(x, y, z)$ is greater than degree of freedom of $\overline{U}_{n-1}(x, y, z)$ and the Taylor expansion of U at the point i is given by:

$$U = U_i + \left.\frac{\partial U}{\partial x}\right|_i (x - x_i) + \left.\frac{\partial U}{\partial y}\right|_i (y - y_i) + \left.\frac{\partial U}{\partial z}\right|_i (z - z_i) \ldots \quad (2)$$

It is shown that,

$$e_i(x, y, z) = O(h^{p+1}), h \to 0 \quad (3)$$

Where: h denotes the maximal size (length) of the element and p the order of the element[4].

Equation (3) shows that in the FEM linear formulation, the flux evaluated within an element is constant and the corresponding error in the fields is e_i = O (h). By the interpolation theory(Figure-1), the flux at a given node is determined by averaging the fluxes of neighboring elements having this node in common; and so we obtain errors O (h^2) at all nodes[1,3]. Around a given node, the local error is defined as follows[4]:

$$e_i = \int_{\Omega_i} (D - D_s) d\Omega \quad (4)$$

Generally, in the nodal classic linear Finite Element Method, the interpolation functions are the same as the simplex coordinates ς_k, k = 1, …, d+1, of a given point Pin side an element e, where d denotes the space dimension. In this case the flux density $\vec{D}$ in equation (4) determined directly from the shape function in scalar field problems is given by the following formula:

$$\vec{D} = \alpha \vec{\nabla} U = \alpha \left(\sum_{k=1}^{d+1} U_k \vec{\nabla} \varsigma_k\right) \quad (5)$$

Where: U denotes the unknown scalar function, U_k, k = 1, …, d+1,the value of the unknown function U at the node k of the element, and α a parameter associated with the physical properties of the domain.

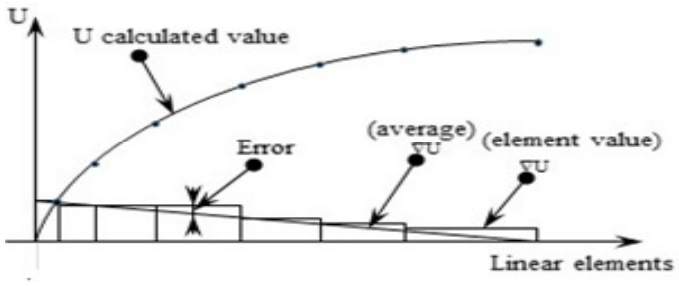

Figure-1: One -dimensional interpolation theory.

The finite element approach in vector field problem show ever relies on basis vector element functions[2, 5]. There are many ways of defining these functions but the following method for d-Simplexes is used in this paper[2]:

$$\vec{N}_n = L_n\left(\varsigma_i\vec{\nabla}\varsigma_j - \varsigma_j\vec{\nabla}\varsigma_i\right) \quad (6)$$

Where: n = 1, 2, ..., n are the edge numbers, i and j $\in$ {1, 2, …, d+1} are the vertex numbers, and L_n, is the length of the n^{th} edge of the element. The flux density $\vec{D}$ in equation (4) determined directly from the shape function in case of magnetic field problems[2,6,7], is thus obtained by the following equation:

$$\vec{D}=\vec{\nabla}\times\vec{U}=\sum_{n=1}^{N} 2U_nL_n(\vec{\nabla}\varsigma_i\times\vec{\nabla}\varsigma_j) \quad (7)$$

The vector $\vec{U}$ in equation (7) denotes the unknown vector function (vector potential in magnetic field problems for example), U_n, n = 1, 2, ..., n are the tangential component of the vector function along the n^{th} edge of the element.

The entity $\vec{D}_s$ in equation (4) represents the average nodal flux density of the area defined by the elements having in common node i of Figure-2 (region around i). In order to generalize the method for any point P of a given element, the local error e_i in equation (4) is replaced by

$$E_e = \sum_{i=1}^{d+1} \varsigma_i e_i \quad (8)$$

Where: d represents the spatial dimension and ς_i, $1 \le i \le d+1$, barycentric coordinates of the point P.

Concept of multi-edge

Definition of Multi-Edge: A portion of curve C approximated by successive segments of lines S_n, $C = \Sigma S_n$, n =1, ..., N, joining two vertices of a linear element is termed Multi-Edge. A segment of line S_n is a virtual edge of a virtual element which may be generated if needed and N is the number of possible virtual edges which can be generated. For example the circular arc boarded by the points 2 and 3 (Figure-3) is represented by the segments of line S_1 = [2 9], S_2 = [9 10] and S_3 = [10 3].

Two main reasons led to the introduction of the concept of Multi-Edge: i. Practically it's impossible to represent non-polynomial curves by polynomial elements such that, there will be no "slivers" of the domain uncovered by an element or to eliminate extra slivers added to it[1]. ii. To be able to refine the mesh adaptively in the areas where boundary condition of a third kind is applied in order to reduce discretization errors leading to boundary mismatch problems in that area.

With this concept, the faces of an element lying along the boundaries could be represented by a special structure which could be compared to multiplex cable in data and communication networks. This element will have normal nodes and virtual nodes or normal edges and virtual edges. For example in Figure-3, the normal representation of the element 2 is {0, 2, 3} and its full representation is {0, 2, 9, 10, 3}.

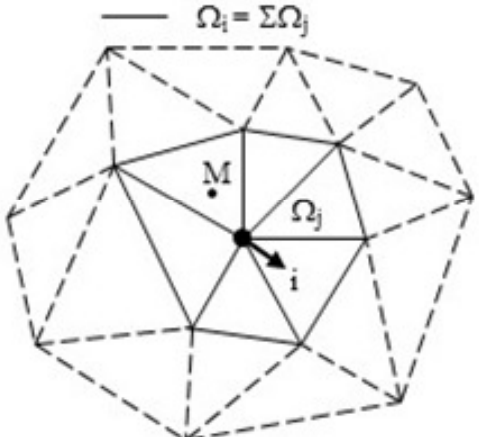

Figure-2: node i in its region of support (2-dimensional case).

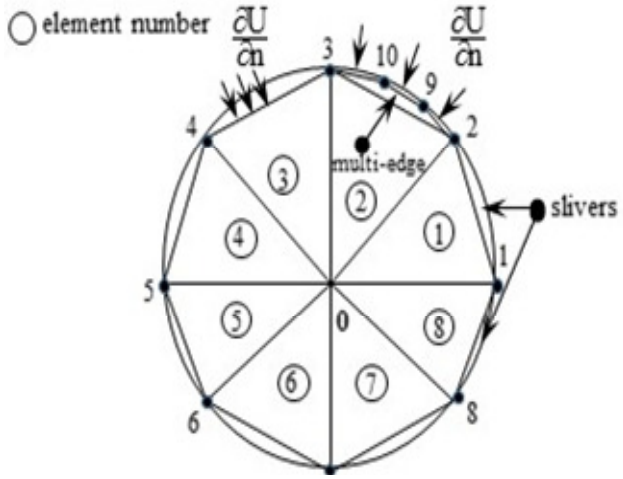

Figure-3: Multi-edge definition.

In fact a Multi-Edge element is identified as an object with d-Simplex object inheritance, where virtual nodes or virtual edges are automatically generated when needed. The definition of a Multi-Edge Element Class may look like:

```
Multi-Edge Element Class: public d-Simplex{
NewPoints Array;
NewEdges Array;
GenerateNewPoints();
GenerateNewEdges();
…..
};
```

The manner in which this virtual edges or nodes will be inserted progressively in mesh when necessary, will be presented in the following section.

h-Adaptive mesh generation: The adaptive methods are brought into the numerical analysis techniques such as the Finite Difference Method (FDM), the FEM and the Boundary Element Method (BEM) in order to use computer resources (for example memory) more efficiently. In many cases, the results of only a few regions for a given domain occupied by a system to be analysed are of interest[1,8,9]. In some cases, before better numerical approximation results could be achieved, a high degree of freedom density must be introduced in some special regions.

In the h-adaptive process, the size of the elements of interest is reduced in the manner that, the length of the maximal edges h_{max} of all elements in that region is also reduced (requirement $h_{max} \rightarrow 0$). This method is also called mesh refinement. The mesh refinement process in this paper relies on two concepts: subdivision of a d-Simplex and construction of new Multi-Edge elements through an old one.

The regions of interest, where the size of elements must be decreased, are defined by the error indicators as presented above in the equations (4 and 8).The regions are either the region of support of a node (Figure-2) or of an element (Figure-4).

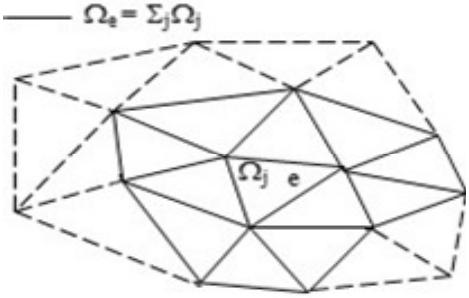

Figure-4: An element e in the region of support.

If e is the element in which the detected error is not acceptable, then e and all the elements which share nodes with it form a local region Ω_e, called region of support of e (Figure-4).

The task of reducing the size of elements in the region of support of an element e is performed in two steps. The first step is subdividing an element e and its neighbours and the second step is the shape regulation of the new resulting elements to get a reasonable mesh for Ω_e.

Subdivision of a d-Simplex: The method of subdividing an element is based on analysing the size of the element. This method was actually developed for an element which does not have any face lying along curved boundaries of the domain. This technique is used in a simplified form and adapted to treat elements with Multi-Edge structure.

An element is subdivided according to the following properties: i. Near equilateral; ii. The longest edge is greater or equal the double of the shortest edge; iii. If it does not satisfy any of the two conditions above; iv. Possesses Multi-Edge structure.

Subdivision of a 2-Simplex: Suppose the element to be subdivided is e = {I, J, K}, where I, J and K denote the vertices of the element. If the element satisfies the condition a), the subdivision is done by generating points at the middle of the edges. The M_i's denote the middle points (Figure-5(a)).

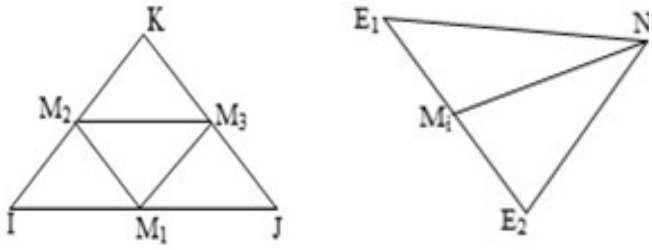

(a) (b)

Figure-5: Reference element e near equilateral case a): (a) sub-division of e, (b) sub-division of a neighbour element of e.

In this case the element of reference is subdivided into 4 elements {I, M_1, M_2}, {J, M_1, M_3}, {K, M_2, M_3}, and {M_1, M_2, M_3}. Any neighbour triangle e_n = {E_1, E_2, N} sharing common edge [E_1, E_2] with the element is then divided into two as in Figure-5(b). The new elements resulting from e_n can be written as

{E_1, M_i, N} and {E_2, M_i, N} i∈{1, 2, 3}.

If the element possesses the property b) a point is generated in the middle of the longest edge and it is subdivided into two new elements as in Figure-6(a). The neighbour element which shares this edge with the element of reference is also subdivided in the same manner (Figure-6(b)).

If the element has the property c) then a Gauss point M is generated and three new elements are formed (Figure-7(a)). The new elements can be written as {I, J, M}, {I, K, M} and {J, K, M.}.

If the element is with Multi-Edges (property d)), one of the free points (virtual node of the mesh) say N_1 is inserted in the system, then two new elements are generated and one external edge is replaced by two (Figure-7(b)). The new elements can be represented as {I, N_1, K} and {N_1, N_2, J, K}.

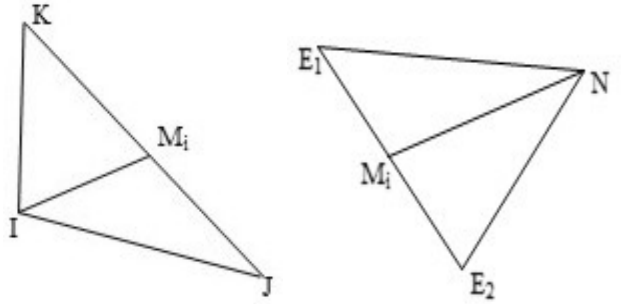

(a) (b)

Figure-6: The longest edge of the reference element e is greater or equal the double of the shortest edge case b): (a) sub-division of e, (b) sub-division of a neighbour element of e.

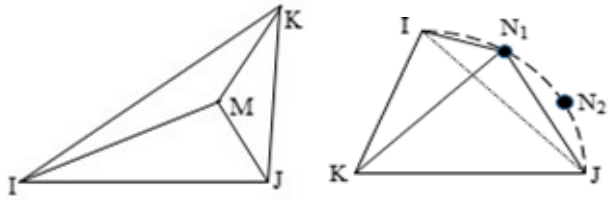

(a) (b)

Figure-7: Case c): Reference element e does not satisfy the conditions a) and b): (a) sub-division of e. case d): Reference element e possesses Multi-Edge structure: (b) construction of new Multi-Edge elements from e.

Hence N_1 is no more a virtual node and will be treated as a new generated point. In fact if there are many free points in the element, the error indicator has to inform the mesh refiner which optimal point to be inserted.

Subdivision of a 3-Simplex: The process of subdividing a given 3-Simplex is just three-dimensional approach of the methods presented above. The manners which the elements are subdivided in cases a), b) and d) are shown figures (Figure**-**8(a, b), Figure**-**9(a, b), Figure**-**10(a, b, c)):

In case a) the element of reference e = {I, J, K, L} is subdivided in 8 new elements (Figure-8 (a)) : {I, M_1, M_2, M_3}, {J, M_1, M_4, M_5}, {K, M_2, M_4, M_6}, {L, M_3, M_5, M_6}, {M_1, M_2, M_3, M_5}, {M_1, M_2, M_4, M_5}, {M_2, M_4, M_5, M_6}, and {M_2, M_3, M_5, M_6} and any neighbour element sharing common facet with it is divided into 4(Figure-8 (b)).

In case b) the element of reference e = {I, J, K, L} is subdivided in 2 new elements (Figure-9 (a)):{I, J, M, L}, {J, K, M, L}and any neighbour element sharing common edge with it is also divided into 2 (Figure-9 (b)).

In case d) the element of reference e = {I, F1, F2, F3} is destroyed and replaced by 4, 3 or 2 new elements according to the size of the external edges: { I, F_1, N_1, N_2}, {I, F_2, N_1, N_3}, {I, F_3, N_2, N_3}, and {I, N_1, N_2, N_3}(Figure-10(a)), { I, F_1, N_1, N_2}, {I, F_2, N_1, F_3}, and {I, F_3, N_1, N_2}}(Figure-10(b)), { I, F_1, N_1, F_3} and {I, F_2, N_1, F_3}(Figure-10(c)).

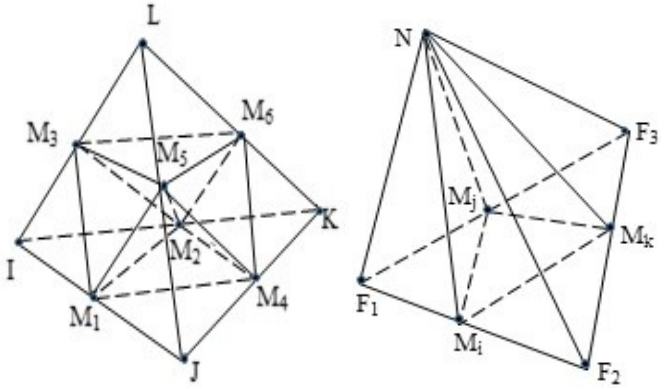

(a) (b)

Figure-8: Reference element e near equilateral case a): (a) sub-division of e, (b) sub-division of a neighbour element of e.

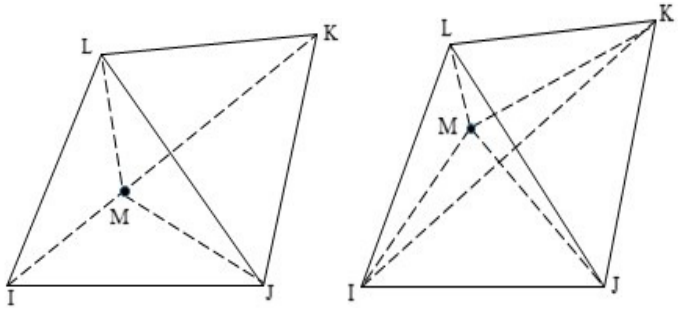

(a) (b)

Figure-9: The longest edge of the reference element e is greater or equal the double of the shortest edge case b): (a) sub-division of e, (b) sub-division of a neighbour element of e.

d-Simplex Shape Regulation in its Domain of Support: The new elements generated for the domain of support of element e (Figure**-**4) have to be controlled if they satisfied the following condition:

All elements must converge towards the equilateral or avoid generating elements of small internal angles, this to minimize the errors of resolution. It is said that finite element resolution errors are inversely proportional to the sine of the smallest internal angles[2,15].

In addition to the previous condition, the concept of zones of a d-Simplex-face point is introduced to ensure the regularity of any element in its support area. This concept consists in saying that, for each facet of an element, a special zone is predefined by the structure of the element. If the neighboring point of this facet is in this zone, the facet can be considered as regular[15].

The neighbor point of a facet of a d-Simplex is the n^{th} vertex of the neighboring element e_n that does not belong to e. For example in the figure (Figure-11) N is defined as a point close to the facet named face-k. In general, a k-zone of a k-face of a d-simplex is a semi-opened sub-zone of the k-zone, delimited by the subspaces of dimension d-1 supporting the facets of the d-simplex[15].

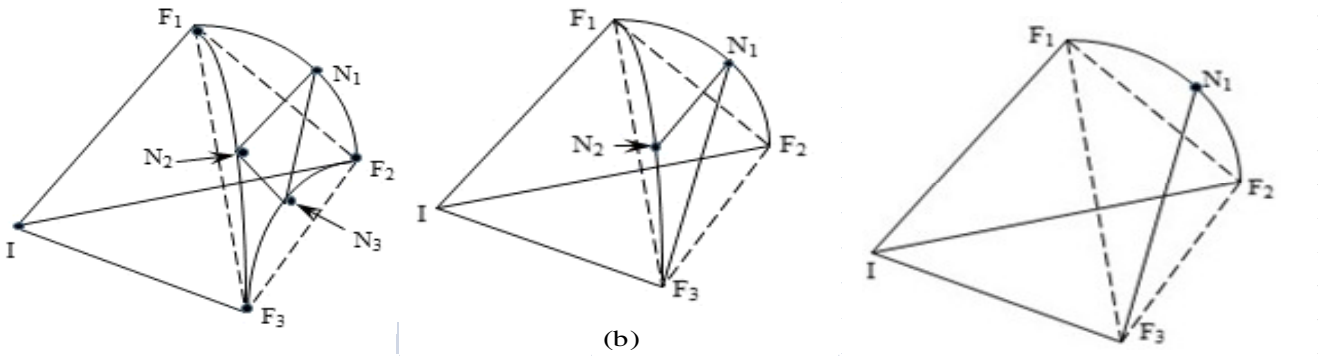

Figure-10: Reference element e possesses Multi-Edge structure case d): (a) construction of 4 new Multi-Edge elements from e, (b) construction of 3 new Multi-Edge elements from e, (c) construction of 2 new Multi-Edge elements from e.

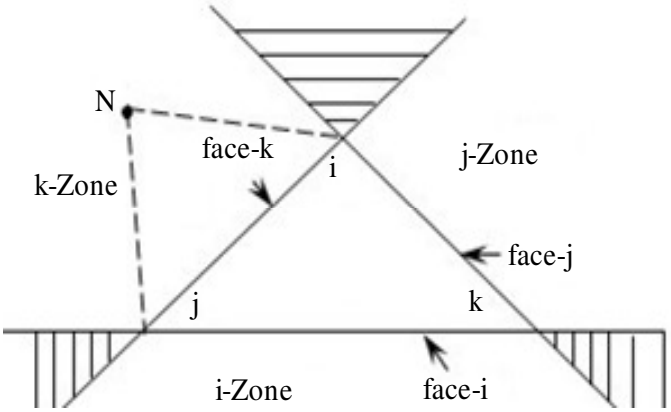

Figure-11: Acceptable region of neighbour points.

Indeed it is easy to see that any point N in this k-zone forms with the face-k of the d-simplex e a non-degenerate d-simplex e_n = {face-k, N} if the distance between this facet and the point N is acceptable. In other words, the point N must not be too far and not too close to this facet. In order to obtain an optimal k-zone two delimiting spheres of the facet are introduced. The first is the circumscribed d-sphere of the d-simplex e and the second a sphere B_R having the same center as the d-sphere but with a radius R greater than the radius r (Figure-12). The zone in the neighborhood of point N is defined by

$$FNPZ_k = \text{k-Zone} \cap B_r \cap B_R \tag{9}$$

for a k-face of an element[15].

The centre C and the radius r of the circumscribed d-sphere B_r of the d-simplex e are defined as

$$\begin{bmatrix} C^1 \\ \vdots \\ C^d \end{bmatrix} = 2 \begin{bmatrix} p_1^1 - p_2^1 & \cdots & p_1^d - p_2^d \\ \vdots & \vdots & \vdots \\ p_1^1 - p_{d+1}^1 & \cdots & p_1^d - p_{d+1}^d \end{bmatrix}^{-1} \begin{bmatrix} \sum_{i=1}^{d} \left(p_1^i\right)^2 - \left(p_2^i\right)^2 \\ \vdots \\ \sum_{i=1}^{d} \left(p_1^i\right)^2 - \left(p_{d+1}^i\right)^2 \end{bmatrix} \tag{10}$$

$$r^2 = \sum_{i=1}^{d} \left(p_1^i - C^i\right)^2 \tag{11}$$

where: P_i, i = 1, …, d+1, are the vertices of the simplex, p_i^n, n = 1 , …, d, are their Cartesian co-ordinates and , C^n, n = 0, 1, ..., d, are the Cartesian co-ordinates of the centre C. The choice of the radius R of the sphere depends on the optimal size of the transition elements one wants to have approximately in the region of interest. Here $R = \alpha r, \alpha > 1$, where $\alpha \in$ [15].

Now a k-face of an element is admissible if its neighbor point N belongs to FNPZk. In the case where the condition is not satisfied then, it's must be checked, if N ∈ B_r or not. If N ∈ B_r then the 'swapping rule' is used to reorder the elements otherwise a new point is generated in the FNPZk for this facet[9, 10, 15].

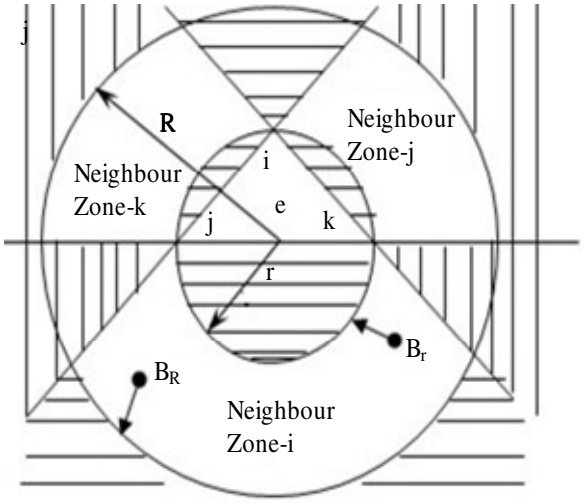

Figure-12: Acceptable region of neighbour points.

The h-Adaptive approach adopted in this paper is summarised in Figure-13. The h-Adaptive method used to solve the magneto-thermal problem treated in[11] is summarized as in Figure-14:

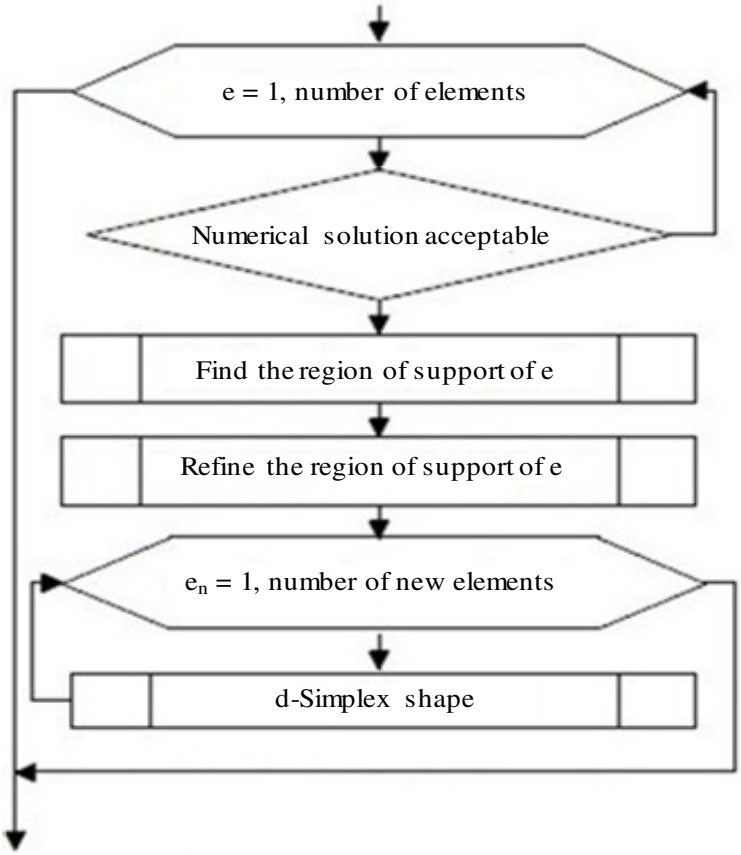

Figure-13: Refinement of the region of support of each error element.

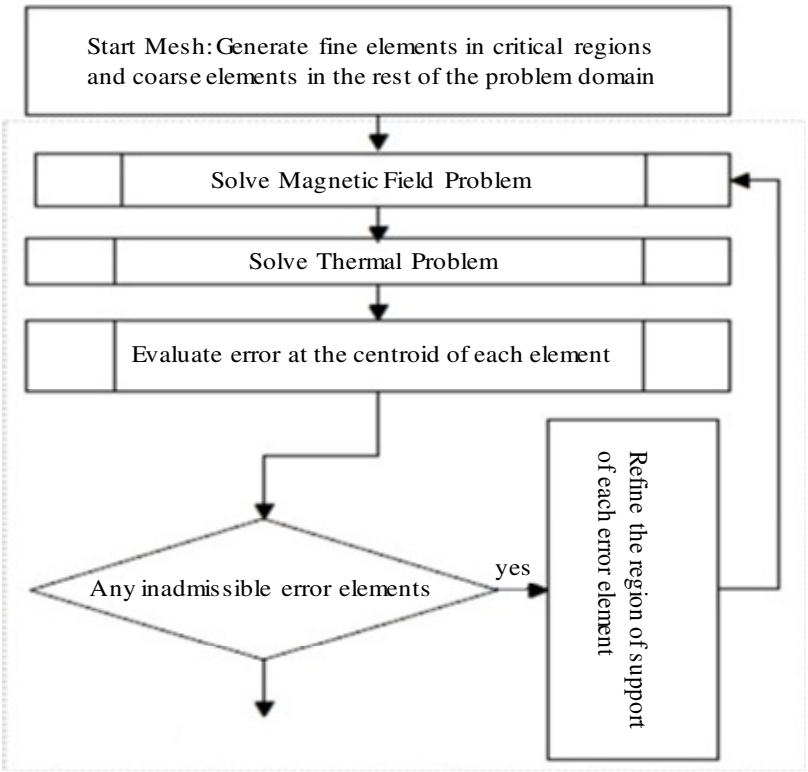

Figure-14: Summary.

Results

Slot cut in all armature of a motor: A problem treated by P. P. Silvester and R.L. Ferrari has been considered. The example relies on a slot cut in all armature of a motor (Figure-15), which is supposed to represent detail from the simplified whole motor cross-section[12].

H-shaped copper bus-bar: Another problem treated by P. P. Silvester and R.L. Ferrari has been considered to check the validity for the FEM analysis of diffusion phenomena[12]. The problem consists of an H-shaped copper bus-bar with overall dimensions 60 mm x 60 mm carrying current at domestic power frequency. The skin depth in copper at 50Hz is about 9mm, so that the calculation of the field penetration into the conductor and the transverse current distribution requires a fully eddy current treatment not readily effected analytically. Figure-16(a) shows the overall geometry concerned. Also an artificial closure was created at a circular boundary of radius 100mm, on the basis that at such a distance the field lines were expected to form a circular pattern regardless of local irregularities in the conductor outline. Thus a Neumann boundary condition was assumed on the symmetry axes, ensuring that the computed field lines intersected these lines at right angles, whilst it was permissible arbitrarily to assign A = 0; at the 100mm-radius circular boundary.

Problem introduced by Webb and Forghani: The problem was considered to evaluate the relative performance of their hierarchical tetrahedron[13]. The model is represented by a magnetic circuit which is driven by a coil having a uniform current density for a supply current of 1A. A copper block (Figure-15) is placed in the air gap of this magnetic circuit having the following characteristics: i. the relative permeability of the non-conductive iron: 1000; ii. the conductivity of copper: 5.7x107 Sm^{-1}; iii. the frequency set: 177.7565 Hz.

Over the entire domain where the physical phenomenon is taking place, the dissipated power P and the stored magnetic energy E (Figure-17) are evaluated at each time step as follows:

$$P = \int_{\Omega_c} \sigma^{-1} \mathbf{J}^2 d\Omega \quad (13)$$

$$E = \frac{1}{2} \int_{\Omega_t} \frac{\mathbf{B}^2}{\mu} d\Omega \quad (14)$$

Where: **J** denotes current density, **B** represents the magnetic flux density, Ω_c denotes the region occupied by the copper block and Ω_t is the whole domain where the physical phenomenon is taking place.

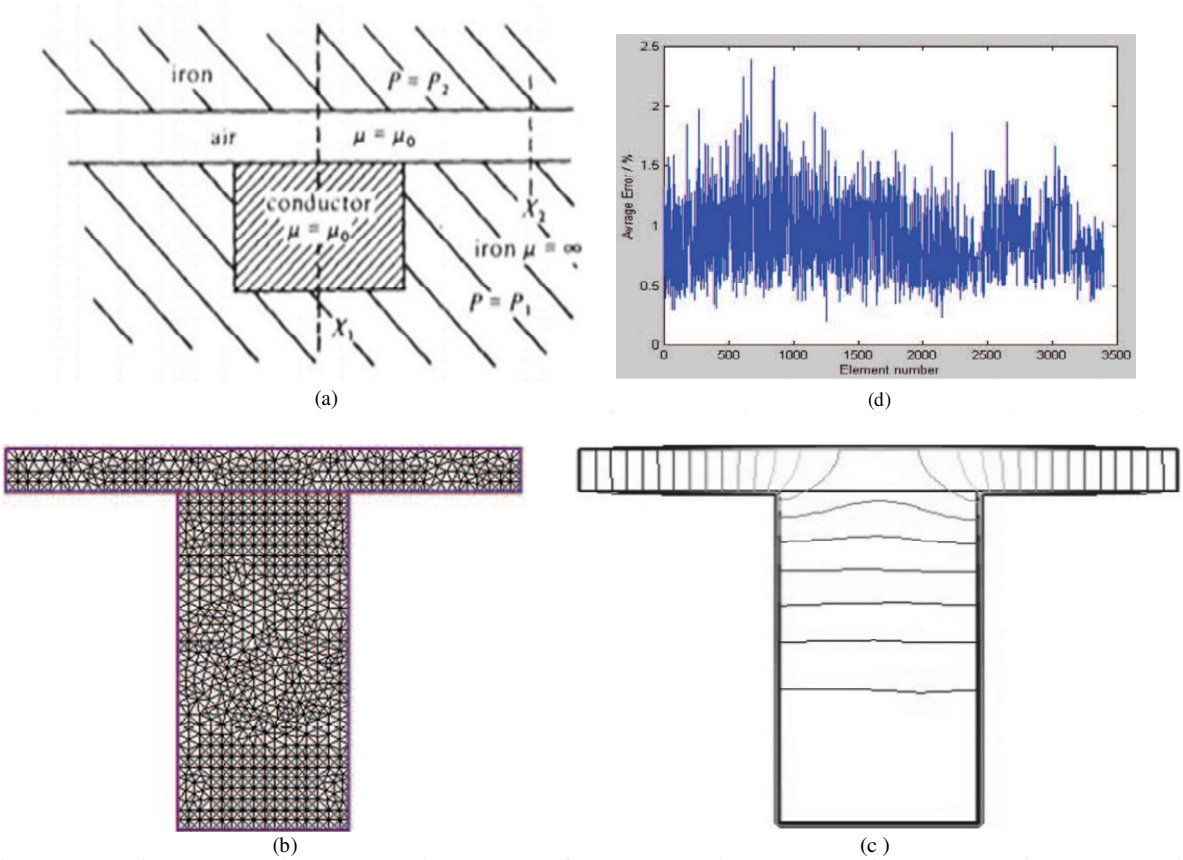

Figure-15: (a) Armature slot in an electric motor[12], (b) Triangular finite element representation of the slot problem: 2245 Elements, 1213 nodes, (c) Finite element solution of the electric machine slot problem, (d) Average Error computed.

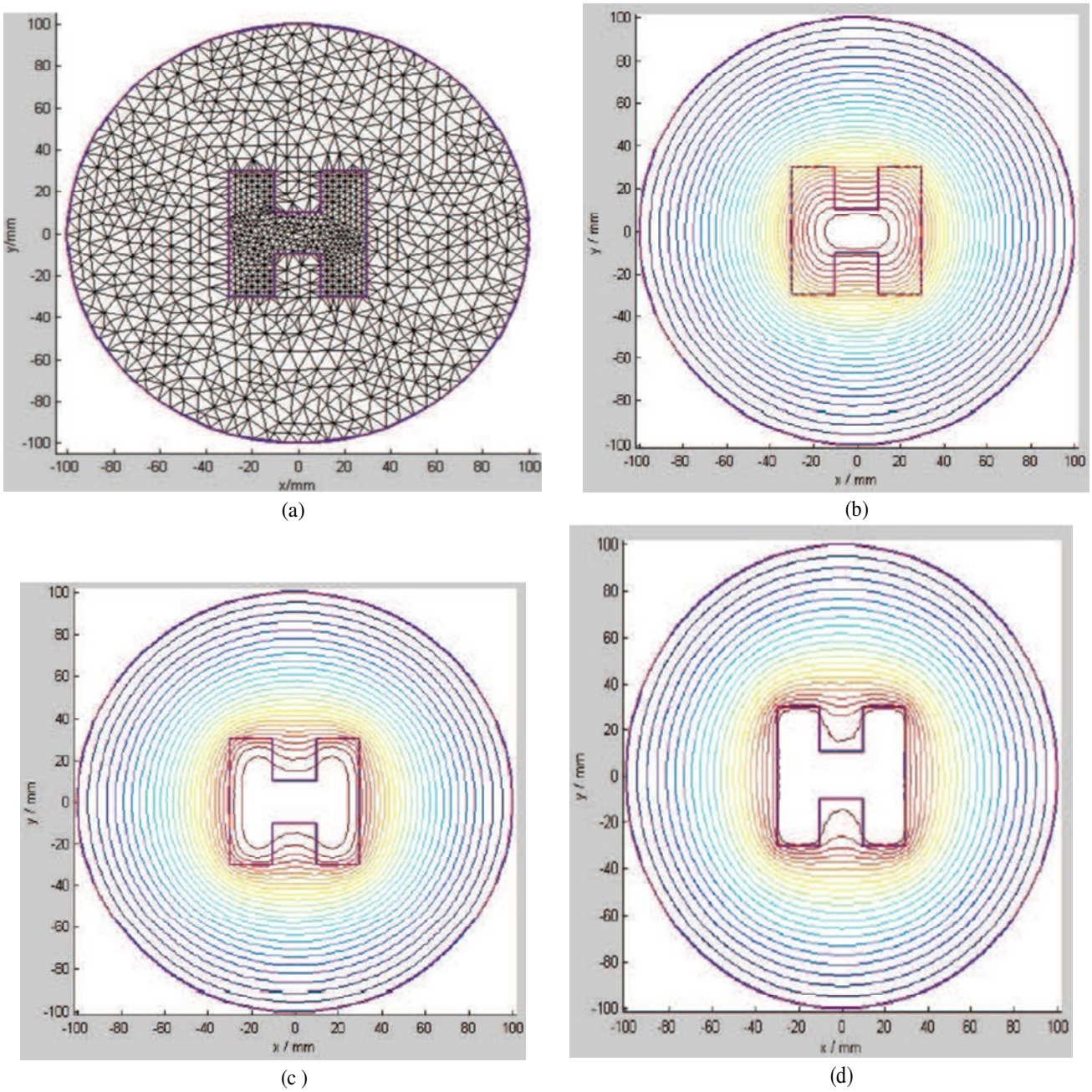

(a) (b)

(c) (d)

Figure-16: (a) Triangular finite element representation of the problem: 1273 nodes and 2448 elements, (b) contour plots of |A|, representing magnetic flux lines at5 Hz, 1213 nodes, (c) contour plots of |A|, representing magnetic flux lines at 50 Hz, (d)contour plots of |A|, representing magnetic flux lines at 200 Hz.

Problem of TEAM Workshop: The distribution of the temperature (measured in °C) of the aluminum plate in the problem 7 (Figure-18)[14].

Conclusion

In any numerical analysis to obtain an appreciable approximate resolution of the physical phenomena one proceeds by the minimization of the errors. This minimization of numerical errors is considered as the basis of analysis in this article. By the finite element method an approach to solve the problem was made using an h-adaptive mesh process. The goal is to show that classical linear finite elements can be used to find solutions for many physical phenomena. Localized error minimization criteria with the Multi-Edge concept and the use of the h-adaptive mesh allowed us to obtain significant numerical results while considerably reducing the computation time. Practical examples were taken into account to validate the localized error usage by methods proposed in this article.

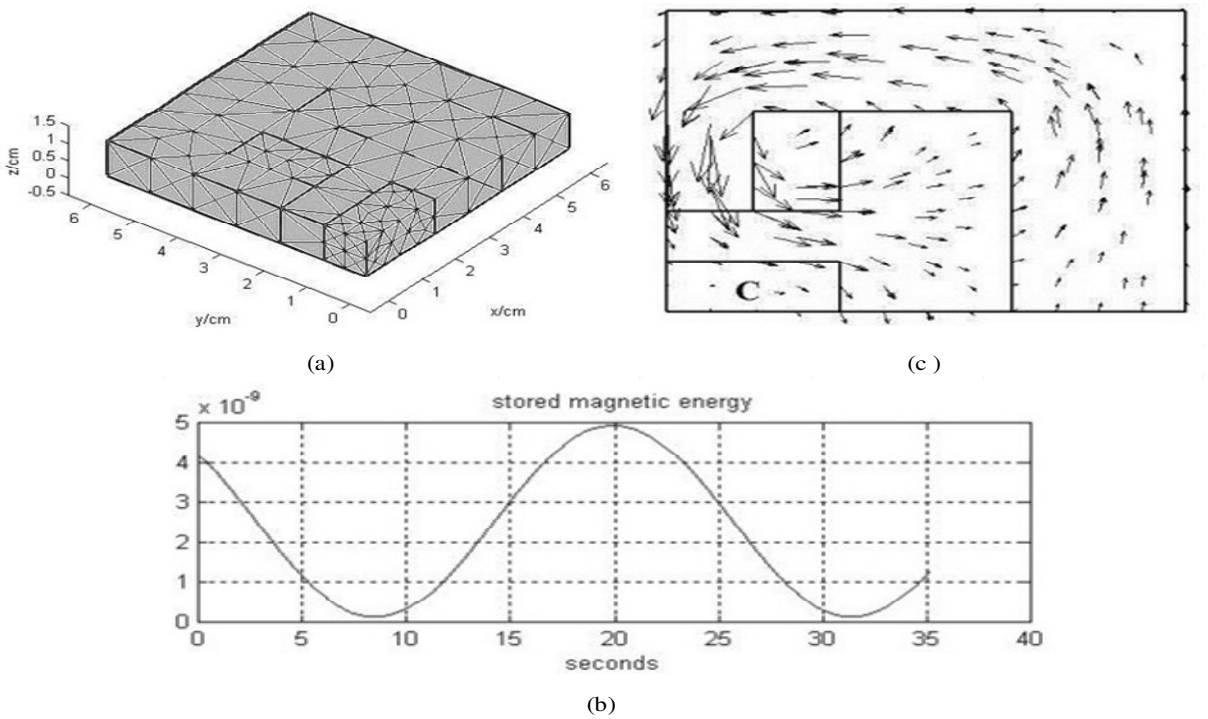

(a) (c)

(b)

Figure-17: (a) 3D FEM model, (b) accumulated magnetic energy, (c) Representation of magnetic flux density vectors at nodes in a quarter-cross section of the copper block C in 3D.

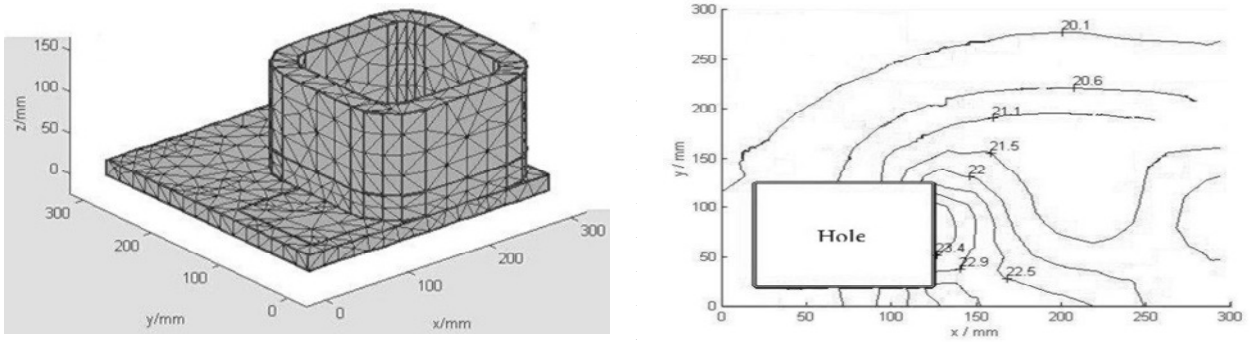

(a) (b)

Figure-18: (a) 3D FEM model, (b) Representation of the temperature distribution curves on the top of the plate at time t = 67s.

Acknowledgement

We thank Mawuli AZIADEKEY, PhD, Professor of Agronomic Sciences (Ecole Supérieure d'Agronomie,University of Lomé) and Essowè Komlan ESSIZEWA, PhD., Professor in Sociolinguistics (Dean of Faculty of Arts and Languages University of Lomé, TOGO) for reading and suggestions during the drafting of this article.

References

1. David Burnnett (1987). Finite Element Analysis from Concept to Applications. Addison-WesleyPub. Co., US, 1-844. ISBN: 9780201108064
2. Jin J.M. (2014). The Finite Element Method in Electromagnetics. Wiley-IEEE Press, US, 1-876. ISBN: 978-1-118-57136-1
3. Binns K.J., Trowbridge C.W. and Lawrenson P.J. (1992). The analytical and numerical solution of electric and magnetic fields. Wiley-Blackwell, US, 1-486. ISBN-10: 0471924601, ISBN-13: 978-0471924609
4. Biddlecombe C., Simkin J. and Trowbridge C. (1986). Error analysis in finite element models of electromagnetic fields. *IEEE Transactions on Magnetics*, 22(5), 811-813.
5. Tanner D.R. and Peterson A.F. (1989). Vector expansion functions for the numerical solution of Maxwell's

equations. *Microwave and Optical Technology Letters*, 2(9), 331-334.

6. Yan S. and Jin J.M. (2015). Theoretical formulation of a time-domain finite element method for nonlinear magnetic problems in three dimensions. *Progress In Electromagnetics Research*, 153, 33-55.

7. Jiao D., Ergin A.A., Shanker B., Michielssen E. and Jin J.M. (2002). A fast higher-order time-domain finite element-boundary integral method for 3-D electromagnetic scattering analysis. *IEEE Transactions on Antennas and Propagation*, 50(9), 1192-1202.

8. Yan S., Lin C.P., Arslanbekov R.R., Kolobov V.I. and Jin J.M. (2017). A Discontinuous Galerkin Time-Domain Method With Dynamically Adaptive Cartesian Mesh for Computational Electromagnetics. *IEEE Transactions on Antennas and Propagation*, 65(6), 3122-3133. DOI: 10.1109/TAP.2017.2689066.

9. Kost A. and Janicke L. (1992). Universal generation of an initial mesh for adaptive 3-D finite element method. *IEEE transactions on magnetics*, 28(2), 1735-1738.

10. Watson D.F. (1981). Computing the n-dimensional Delaunay tessellation with application to Voronoi polytopes. *The computer journal*, 24(2), 167-172.

11. Kpogli K. and Kost A. (2003). Local error estimation and strategic mesh generation for time-dependent problems in electromagnetics coupled with heat conduction. *IEEE transactions on magnetics*, 39(3), 1701-1704.

12. Silvester P.P. and Ferrari R.L. (1983). Finite Elements for Electrical Engineers. Cambridge University Press,United Kingdom, 1-499. ISBN 10 : 0-521-44953-7

13. Webb J.P. and Forghani B. (1995). T-omega method using hierarchal edge elements. *IEE Proceedings-Science, Measurement and Technology*, 142(2), 133-141.

14. Turner L.R., Davey K., Ida N., Rodger D., Kameari A., Bossavit A. and Emson C.R.I. (1988). Workshops and problems for benchmarking eddy current codes (No. ANL/FPP/TM-224). Argonne National Lab., IL (USA).

15. Komla Kpogli, Sibiri Wourè-Nadiri Bayor, Ayité Senah Akoda Ajavon, Kokou Tcharie and Arnulf Kost (2017). Optimal Meshing of Structured Boundary Domains in Numerical Analyses. *American Journal of Engineering and Applied Sciences*, 10(4), 835-848. Doi: 10.3844/ajeassp.2017.835.846.